5-31-2011

Induced p-wave superfluidity in strongly interacting imbalanced Fermi gases

Kelly R. Patton
Louisiana State University

Daniel E. Sheehy
Louisiana State University

Induced p-wave superfluidity in strongly interacting imbalanced Fermi gases

Kelly R. Patton* and Daniel E. Sheehy†

Department of Physics and Astronomy, Louisiana State University, Baton Rouge, Louisiana 70803

(Dated: November 19, 2010)

The induced interaction among the majority spin species, due to the presence of the minority species, is computed for the case of a population-imbalanced resonantly-interacting Fermi gas. It is shown that this interaction leads to an instability, at low temperatures, of the recently observed polaron Fermi liquid phase of strongly imbalanced Fermi gases to a p-wave superfluid state. We find that the associated transition temperature, while quite small in the weakly interacting BCS regime, is experimentally accessible in the strongly interacting unitary regime.

PACS numbers: 05.30.Fk, 03.75.Ss, 67.85.-d, 32.30.Bv

The extraordinary controllability of cold atomic gases has yielded a wide range of interesting phases of matter, including a bosonic Mott insulator and a paired superfluid state of two species of atomic fermions [1, 2]. In the latter setting, experiments have demonstrated control of both the interspecies interactions and the relative density of the two spin states [3, 4], with the latter experimental knob being deleterious to pairing and superfluidity, which favors an equal density of the two species.

Thus, experiments on such imbalanced Fermi gases can probe the stability of superfluidity in a correlated system and therefore may shed light on the tendency towards pairing in related systems, such as electronic superconductors. The phase diagram of imbalanced Fermi gases is quite rich [5, 6], possessing regions of imbalanced superfluidity, phase separation, normal Fermi liquid, and (possibly, though not yet observed) a region of exotic Fulde-Ferrell-Larkin-Ovchinnikov (FFLO) superfluidity [7].

Our present focus is on the strongly imbalanced region, when the polarization $P = \frac{n_\uparrow - n_\downarrow}{n_\uparrow + n_\downarrow}$ (with n_σ the density of fermion species σ) is close to unity, with a small density of spins-$\downarrow$ immersed in a spin-$\uparrow$ Fermi sea. Experiments in this regime [8, 9] have found results consistent with the formation of spin polarons [10], in which a cloud of spins-$\uparrow$ gather around each spin-$\downarrow$, leading to a polaron Fermi liquid state [11–13].

The polaron theory of the strongly imbalanced Fermi gas predicts that both the spins-$\uparrow$ and spins-$\downarrow$ are Fermi liquids, exhibiting sharp Fermi surfaces at low temperature T. However, general arguments due to Kohn and Luttinger (KL) [14, 15] predict that such Fermi surfaces must be unstable to other ordered states as $T \to 0$. A natural question then emerges: What is this ordered state for imbalanced Fermi gases? Since the imposed imbalance (and concomitant Fermi-surface mismatch) precludes s-wave singlet interspecies pairing, one instead expects triplet (likely p-wave) *intraspecies* pairing [14–16] of the spin-$\uparrow$ and spin-$\downarrow$ fermions.

In this Rapid Communication we develop a theoretical

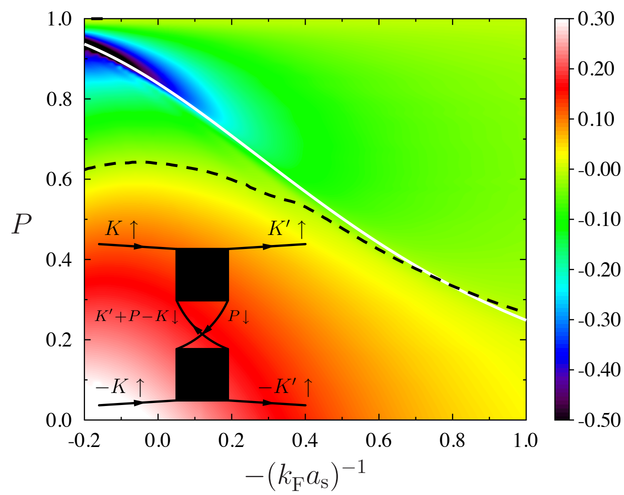

FIG. 1: (Color online) The p-wave channel of the effective interaction, determined by the diagrammatic inset, between majority spins, $v^{\ell=1}(k_{\rm F\uparrow}, k_{\rm F\uparrow})$, multiplied by the Fermi-energy density of states $N_\uparrow(\epsilon_{\rm F\uparrow})$, as a function of the density imbalance P and s-wave scattering length a_s, is shown. Here, $k_{\rm F} = (k_{\rm F\uparrow} + k_{\rm F\downarrow})/2$. At large P, above the dashed line, it is *attractive* leading to a p-wave superfluid at temperatures below $T_{\rm c}$. The solid white line labels the location of a line of FFLO quantum critical points. This coincides with the location where $v^{\ell=1}(k_{\rm F\uparrow}, k_{\rm F\uparrow})$ is large.

description of the induced interactions among the majority spin-$\uparrow$ fermions in the presence of a small density of spins-$\downarrow$, over a broad range of interaction and polarization values. We find an attractive effective interaction at the spin-$\uparrow$ Fermi surface, shown in Fig. 1, leading to an instability towards p-wave superfluidity below a transition temperature $T_{\rm c}$, computed below [17]. In the extreme weak coupling Bardeen-Cooper-Schrieffer (BCS) limit, where the s-wave scattering length $a_s \to 0^-$, the p-wave superfluid transition temperature has been computed [16]; unfortunately, it is exceptionally small (in agreement with KL [14]), with $T_{\rm c} \propto \exp[-c/(k_{\rm F\uparrow} a_s)^2]$, where $k_{\rm F\uparrow}$ is the spin-$\uparrow$ Fermi wave vector and c is a constant of order unity. The pairing mechanism is quite simple in this perturbative limit: density fluctuations of one species leads to an attraction between particles of op-

*kpatton@lsu.edu

†sheehy@phys.lsu.edu

posite spin. For spins-↑, this induced interaction is proportional to the spin-↓ density-density correlation function (i.e., the Lindhard function). Although a p-wave superfluid is predicted in the BCS limit, most experiments occur in the unitary region where the interspecies interactions are strong, $|a_s| \to \infty$, invalidating simple perturbative results. Our analysis of induced interactions in the unitary regime involves extending the ladder approximation (known to describe the polaron Fermi liquid regime discussed above) to include subleading classes of Feynman diagrams. As seen in Fig. 1, the predicted effective interaction in the p-wave channel can be quite large near the unitary regime We find a maximum transition temperature of $k_{\rm B}T_{\rm c} \simeq 0.03\epsilon_{{\rm F}\uparrow}$, which is low but not unreasonable given recently reported temperature scales (e.g., Ref. 18).

Our starting point is the standard one-channel model for two species ($\sigma =\uparrow,\downarrow$) of fermion ($c^\dagger_{\mathbf{k}\sigma}$) interacting via an s-wave Feshbach resonance [19]. The Hamiltonian is

$$H = \sum_{\mathbf{k},\sigma} \xi_{\mathbf{k}\sigma} c^\dagger_{\mathbf{k}\sigma} c_{\mathbf{k}\sigma} + \frac{\lambda}{\mathsf{V}} \sum_{\mathbf{k},\mathbf{k}',\mathbf{q}} c^\dagger_{\mathbf{k}+\mathbf{q}\uparrow} c^\dagger_{\mathbf{k}'-\mathbf{q}\downarrow} c_{\mathbf{k}'\downarrow} c_{\mathbf{k}\uparrow}, \quad (1)$$

where $\xi_{\mathbf{k}\sigma} = \epsilon_{\mathbf{k}} - \mu_\sigma$, with dispersion $\epsilon_{\mathbf{k}} = k^2/2m$ ($\hbar = 1$) and chemical potential μ_σ; V is the system volume (henceforth set to unity), and λ is the coupling strength of a short-ranged pseudo-potential, related to the experimentally controllable (via a magnetic field-tuned Feshbach resonance) scattering length a_s via

$$\frac{m}{4\pi a_s} = \lambda^{-1} + \sum_{\mathbf{k}}^{\Lambda} \frac{1}{2\epsilon_{\mathbf{k}}}, \quad (2)$$

where Λ is an ultraviolet cutoff; below we shall take the limit $\Lambda \to \infty$ while $\lambda \to 0^-$, such that a_s remains fixed.

We are interested in the phases of Eq. (1) in the strongly imbalanced limit $P \to 1$ and proceed (in the spirit of mean-field theory) by assuming the presence of a self-consistently determined pairing amplitude $\Delta_\uparrow(\mathbf{k},\omega)$ among the spins-↑, but not the spins-↓ [17]. Under this assumption, the 2×2 spin-↑ Nambu Green's function, in Fourier-Matsubara space, is $\hat{\mathcal{G}}_\uparrow(K) = \begin{pmatrix} G_\uparrow(K) & F_\uparrow(K) \\ F_\uparrow(K) & -G_\uparrow(-K)\end{pmatrix}$, where the four-vector $K = (i\omega_n, \mathbf{k})$. $\hat{\mathcal{G}}_\uparrow(K)$ satisfies the Dyson equation [20] $\hat{\mathcal{G}}^{-1}_\uparrow(K) = \hat{\mathcal{G}}^{-1}_{\uparrow,0}(K) - \hat{\Sigma}_\uparrow(K)$, with bare Green's function $\hat{\mathcal{G}}^{-1}_{\uparrow,0}(K) = \begin{pmatrix} i\omega_n - \xi_{\mathbf{k}\uparrow} & 0 \\ 0 & i\omega_n + \xi_{\mathbf{k}\uparrow}\end{pmatrix}$ and self-energy $\hat{\Sigma}_\uparrow(K) = \begin{pmatrix} \Sigma_\uparrow(K) & -\Delta_\uparrow(K) \\ -\Delta^*_\uparrow(K) & -\Sigma_\uparrow(-K)\end{pmatrix}$. Using the equation of motion [21], the self-energy can be expressed in terms of the two-particle vertex $\hat{\Gamma}$, by

$$\hat{\Sigma}_\uparrow(K) = \lambda\sigma_z \sum_{K_1} G_\downarrow(K_1)\Big[\sigma_0 - \sum_{K_2} \hat{\mathcal{G}}_\uparrow(K_2) G_\downarrow(K+K_1-K_2)\hat{\Gamma}(K_2, K+K_1-K_2, K_1, K)\Big], \quad (3)$$

where σ_0 is the 2×2 identity matrix, σ_z is a Pauli matrix, and $G_\downarrow(K)$ is the scalar spin-↓ Green's function, which satisfies a similar expression, but with a diagonal self-energy (since we assumed the spins-↓ are unpaired). The summation is short for $\sum_K \equiv k_{\rm B}T\sum_{i\omega_n}\sum_{\mathbf{k}}$.

Although Eq. (3) is in principle exact, to make progress we must make a physically motivated approximation for $\hat{\Gamma}$, correpsonding to certain classes of Feynman diagrams. Previous work has analyzed the phases of imbalanced Fermi gases within the t-matrix or ladder approximation [11, 22, 23]. The set of diagrams associated with the ladder approximation also emerges in the large-N approximation [12], in which one generalizes the model to consist of $2N$ species of fermion. Within the present formalism in which $\hat{\mathcal{G}}_\uparrow(K)$ has Nambu structure, these contributions arise from including the ladder plus the maximally crossed self-energy diagrams, sketched in Figs. 2(a) and 2(b), respectively. We first analyze Eq. (3) including only these diagrams. Exchanging λ for a_s using Eq. (2), and keeping only contributions that are finite in the limit $\Lambda \to \infty$, we find a *diagonal* self-energy;

$$\hat{\Sigma}_\uparrow(K) = \sum_Q G_\downarrow(Q)\begin{pmatrix} t(Q+K) & 0 \\ 0 & -t(Q-K)\end{pmatrix}, \quad (4)$$

indicating the absence, at this level, of pairing for the spins-↑. Here,

$$t(K)^{-1} = \frac{m}{4\pi a_s} + \sum_Q G_\downarrow(K-Q)G_\uparrow(Q) - \sum_{\mathbf{q}} \frac{1}{2\epsilon_{\mathbf{q}}}, \quad (5)$$

is the usual scalar t-matrix.

Thus, the contributions from Figs. 2(a) and 2(b) yield an unpaired solution for the self-energy, i.e., a Fermi liquid, as found by previous t-matrix or large-N theories [11, 12, 22, 23]. Given that the KL arguments imply the eventual instability of this state, we now turn to subleading contributions to the self-energy, shown in Fig. 2(c), that possess ladder and crossed-ladder subdiagrams. Again replacing λ for a_s using Eq. (2), we find that these diagrams yield an off-diagonal contribution to

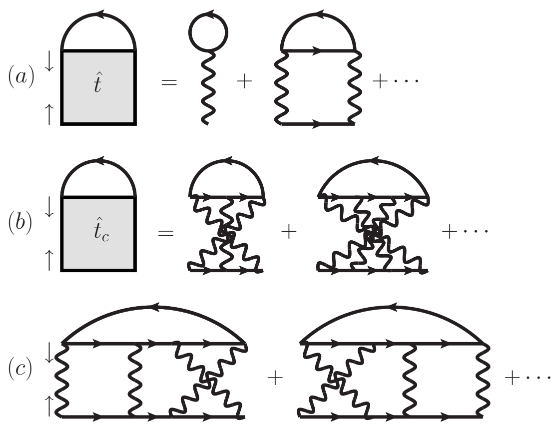

FIG. 2: The ladder (a) and maximally crossed (b) diagrams contributing to the self-energy, which define the ladder $\hat{t}$ and crossed-ladder $\hat{t}_c$ diagrams. The bottom row, (c), shows a subleading class of diagrams with both ladder and crossed-ladder diagrams that lead to a pairing instability. The spin-↑ lines are 2×2 Nambu Green's functions $\hat{\mathcal{G}}_\uparrow(K)$, spin-↓ lines are normal scalar Green's functions $G_\downarrow(K)$, and the wavy lines are $\lambda\sigma_z$.

the self-energy, i.e., a pairing amplitude $\Delta_\uparrow(K)$ given by

$$\Delta_\uparrow(K) = \sum_Q V(K,K')F_\uparrow(K'), \tag{6}$$

$$V(K,K') = \sum_P t(P-K)t(P+K')G_\downarrow(P)G_\downarrow(K'+P-K) \tag{7}$$

Here, $V(K,K')$ is the effective induced interaction among spins-↑; the corresponding Feynman diagram is shown in Fig. 1. In principle, the integral equation (6) must be solved self-consistently along with the diagonal self-energy, Eq. (4). However, we shall we use some physically motivated approximations to simplify our analysis, focusing on the onset of pairing of the spins-↑ at a temperature T_c (above which the system is a Fermi liquid). We assume the presence of a static momentum-dependent pairing order parameter, $\Delta_\uparrow(K) = \Delta_\uparrow(\mathbf{k})$, and neglect the frequency dependence of $V(K,K')$ [15]. For the diagonal components of the self-energy, we simply assume that the chemical potential is renormalized to the Fermi energy via $\mu_\sigma \to \mu_\sigma - \Sigma_\sigma(\mathbf{k}_F^\sigma, 0) = \epsilon_{F\sigma}$ (consistent with the Luttinger theorem [24, 25]). Within these approximations and after analytic continuation the effective interaction takes the form

$$V(\mathbf{k},\mathbf{k}') \approx 2\mathrm{Re}\Big[\sum_{\mathbf{q}} t^{\mathrm{r}}(\mathbf{k}+\mathbf{q},\xi_{\mathbf{q}\downarrow})t^{\mathrm{a}}(\mathbf{q}-\mathbf{k}',\xi_{\mathbf{q}\downarrow}) \times G_\downarrow^{\mathrm{r}}(\mathbf{k}-\mathbf{k}'+\mathbf{q},\xi_{\mathbf{q}\downarrow})n_{\mathrm{F}}(\xi_{\mathbf{q}\downarrow})\Big], \tag{8}$$

where r/a refers to the retarded or advanced quantities and $n_{\mathrm{F}}(\omega)$ is the Fermi distribution function. Equation (6) then simplifies to

$$\Delta_\uparrow(\mathbf{k}) = -\sum_{\mathbf{k}'} V(\mathbf{k},\mathbf{k}')\frac{\Delta_\uparrow(\mathbf{k}')}{2E_{\mathbf{k}'}}\tanh\frac{E_{\mathbf{k}'}}{2T}, \tag{9}$$

with $E_{\mathbf{k}} = \sqrt{\xi_{\mathbf{k}\uparrow}^2 + |\Delta_\uparrow(\mathbf{k})|^2}$, the solution of which requires an understanding of the momentum structure of the effective interaction $V(\mathbf{k},\mathbf{k}')$ in the vicinity of the spin-↑ Fermi surface. The transition temperature T_c for a given angular momentum is found by solving the linearized, in $\Delta_\uparrow(\mathbf{k})$, version of Eq. (9) and projecting onto the relevant channel [19]. Assuming p-wave pairing, one needs the $\ell = 1$ projection of the induced interaction, $v^{\ell=1}(k,k') = \int_0^\pi d\theta\, \sin\theta\cos\theta V(\mathbf{k},\mathbf{k}')$, where θ is the angle between $\mathbf{k}$ and $\mathbf{k}'$. Furthermore, we find via a direct numerical integration of Eq. (8), that $v^1(k,k')$ is only appreciable for k and k' within a range $k_{F\downarrow}$ of each other; this defines an effective bandwidth, of the order of $\epsilon_{F\downarrow}$, over which the induced interaction is nonzero.

The strong induced attraction among the spins-↑, shown in Figs. 1 and 3a, suggest a robust p-wave superfluid at $T \to 0$; to estimate the associated transition temperature T_c we must make further approximations. The remaining momentum integrations in Eq. (9) are sharply peaked at the Fermi surface, yielding the result

$$k_{\mathrm{B}}T_c \approx \frac{2e^\gamma}{\pi}\epsilon_{F\downarrow}\exp\Big[\frac{1}{N_\uparrow(\epsilon_{F\uparrow})v^{\ell=1}(k_{F\uparrow},k_{F\uparrow})}\Big], \tag{10}$$

with γ the Euler gamma constant. We have also found [26] the same result for the transition temperature (and the same effective interaction, Eq. (7)) via a somewhat different approach by considering the Thouless criterion [27] for T_c, determined by the point at which the spin-↑ pair-pair fluctuations in the normal state become unbounded. Within such an approach, Eq. (7) is the irreducible vertex in the particle-particle channel of the Bethe-Salpeter equation [28].

In general, (8) has to be determined numerically, but analytic results can be found for certain limiting cases. In the asymptotic BCS limit $a_s \to 0^-$, the t-matrix $t^{\mathrm{r/a}}(\mathbf{k},\omega) \to 4\pi a_s/m$, and Eq. (8) reduces to the result of Ref. [16] (where, as we have noted, T_c is extremely small). Analytic results can also be obtained in the extremely imbalanced limit, i.e., $k_{F\uparrow}/k_{F\downarrow} \gg 1$. In this limit the t-matrices appearing in Eq. (8) also become independent of $\mathbf{k}$ and $\mathbf{k}'$; $t^{\mathrm{r/a}}(k_{F\uparrow} \pm \mathbf{q}, \xi_{\mathbf{q}\downarrow}) \to \big(\frac{m}{4\pi a_s} - \frac{mk_{F\uparrow}}{4\pi^2}\big)^{-1}$. Evaluating the remaining integral gives

$$k_{\mathrm{B}}T_c \approx \frac{2e^\gamma}{\pi}\epsilon_{F\downarrow}\exp\Big[-\frac{3}{2}\frac{z}{\ln(z)}\Big(\frac{\pi}{2k_{F\downarrow}a_s} - \frac{z}{2}\Big)^2\Big], \tag{11}$$

with $z = k_{F\uparrow}/k_{F\downarrow}$. This formula correctly captures the vanishing of T_c for $P \to 1$, but doesn't adequately capture the peaks shown in Fig. 3, which where found by a direct numerical analysis of Eq. (8). These results indicate the presence of pairing at an experimentally accessible temperature in unitary imbalanced gases.

The peak in the induced attraction, and in T_c, at large P, can be understood by noting that a crucial contribution comes from particle-hole excitations at the spin-↓ Fermi surface. However, particle-hole excitations with a transferred momentum larger than $2k_{F\downarrow}$ are energetically suppressed, so that the associated density response

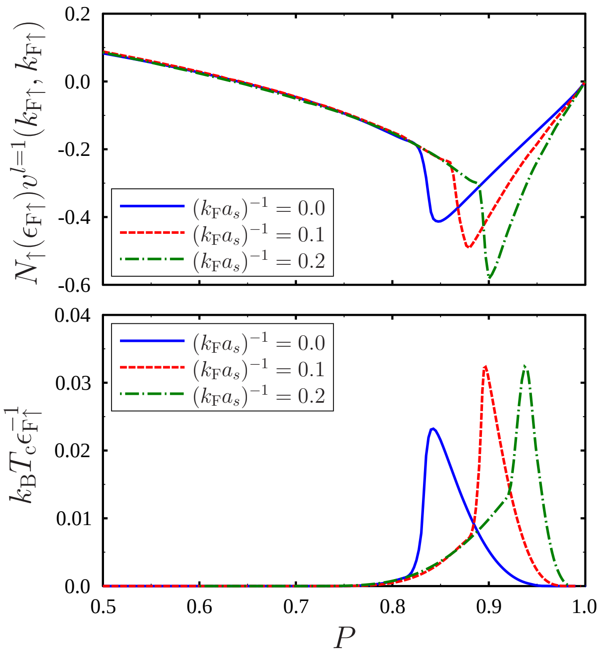

FIG. 3: The top panel shows the $l = 1$ channel of the effective interaction for spin-↑ fermions, times the density of states, as a function of polarization, at unitary and into the BEC side. The bottom panel shows the corresponding p-wave transition temperature, according to Eq. (10), with $\epsilon_{F\uparrow}/\epsilon_{F\downarrow} = [(1+P)/(1-P)]^{2/3}$, via a numerical integration of Eq. (8).

exhibits a strong momentum dependence at $k \simeq 2k_{F\downarrow}$, and a correspondingly large p-wave projected interaction at $k_{F\uparrow} \simeq 2k_{F\downarrow}$, or $P = \frac{k_{F\uparrow}^3 - k_{F\downarrow}^3}{k_{F\uparrow}^3 + k_{F\downarrow}^3} \simeq 0.78$. Near unitarity, the magnitude of this peak is enhanced by the presence of strong fluctuations toward the FFLO phase, signaled by a divergence of the t-matrix at a non-zero wave vector $\mathbf{Q}$, i.e., $t^r(\mathbf{Q}, 0) \to \infty$. To illustrate this, in Fig. 1 the white line shows the P at which a quantum phase transition to the FFLO state occurs; thus, below this line, the p-wave paired phase may undergo a second phase transition to the FFLO.

The confirmation of our scenario will require detecting the onset of p-wave pairing at T_c and the properties of the resulting p-wave superfluid below T_c. This can be done via standard probes of superfluidity, such as the presence of vortices in a rotating cloud [29]. Following general arguments [30–32], we expect a $p_x + ip_y$ ground state, i.e. $\Delta_\uparrow(\mathbf{k}) = \Delta_0 Y_{1,1}(\hat{\mathbf{k}})$. The anisotropic gapping of the spin-↑ Fermi surface should yield a signature in radio-frequency (RF) spectroscopy, which measures the atom transfer rate of one spin species from the interacting system to an unoccupied energy level [33], probing the spectral function. However, we find that the associated peak position in the RF line-shape is at $\omega \simeq \Delta_0(\Delta_0/\epsilon_{F\uparrow})$, a very small energy scale given the smallness of T_c computed above. A more promising route, that we leave for future research, is the question of how the onset of pairing impacts the formation of the spin-↓ polarons (as reflected in, e.g., the spin-↓ RF spectra [8]).

In summary, we have calculated the induced interaction between like atoms in the normal state of an imbalanced two-component Fermi gas. In the absence of any competing instabilities (which certainly occur at smaller P, where the regimes of magnetic superfluidity [34], phase separation and, possibly FFLO phase occur), this interaction leads to the formation of a p-wave superfluid in the majority spin species, with a transition temperature that peaks, for P close to unity, at a few percent of the spin-↑ Fermi energy.

This work has been supported by the Louisiana Board of Regents, under grant LEQSF (2008-11)-RD-A-10.

---

[1] I. Bloch et al., Rev. Mod. Phys. **80**, 885 (2008).
[2] S. Giorgini et al., Rev. Mod. Phys. **80**, 1215 (2008).
[3] M.W. Zwierlein et al., Science **311**, 492 (2006).
[4] G.B. Partridge et al., Science **311**, 503 (2006).
[5] Y. Shin et al., Nature **451**, 689 (2008).
[6] Y. Shin et al., Phys. Rev. Lett. **101**, 070404 (2008).
[7] L. Radzihovsky and D.E. Sheehy, Rep. Prog. Phys. **73**, 076501 (2010).
[8] A. Schirotzek et al., Phys. Rev. Lett. **102**, 230402 (2009).
[9] S. Nascimbène et al., Phys. Rev. Lett. **103**, 170402 (2009).
[10] F. Chevy, Phys. Rev. A **74**, 063628 (2006).
[11] R. Combescot, Phys. Rev. Lett. **98**, 180402 (2007).
[12] M. Veillette et al., Phys. Rev. A **78**, 033614 (2008).
[13] R. Combescot and S. Giraud, Phys. Rev. Lett. **101**, 050404 (2008).
[14] W. Kohn and J. M. Luttinger, Phys. Rev. Lett. **15**, 524 (1965).
[15] J. M. Luttinger, Phys. Rev. **150**, 202 (1966).
[16] A. Bulgac, M. M. Forbes, and A. Schwenk, Phys. Rev. Lett. **97**, 020402 (2006).
[17] Within our theory, the spins-↑ are also predicted to induce pairing among the spins-↓; we find the associated temperature scale to be much lower.
[18] A. Schirotzek et al., Phys. Rev. Lett. **101**, 140403 (2008).
[19] V. Gurarie and L. Radzihovsky, Ann. Phys. **322**, 2 (2007).
[20] A.A. Abrikosov, L.P. Gorkov, and I.E. Dzyaloshinskii, *Methods of Quantum Field Theory in Statistical Physics*, Dover, 1975.
[21] G. Baym and L.P. Kadanoff, Phys. Rev. **124**, 287 (1961).
[22] M. Punk and W. Zwerger, Phys. Rev. Lett. **99**, 170404 (2007).
[23] W. Schneider and M. Randeria, Phys. Rev. A **81**, 053610 (2010).
[24] J.M. Luttinger and J.C. Ward, Phys. Rev. **118**, 1417 (1960).
[25] S. Sachdev and K. Yang, Phys. Rev. B **73**, 174504 (2006).
[26] K.R. Patton and D.E. Sheehy, in preparation.
[27] D.J. Thouless, Ann. Phys. **10**, 553 (1960).
[28] P. Nozières, *Theory of interacting Fermi Systems* (Westview Press, 1997).

[29] M.W. Zwierlein et al., Nature **435**, 1047 (2005).
[30] P. W. Anderson and P. Morel, Phys. Rev. **123**, 1911 (1961).
[31] V. Gurarie, L. Radzihovsky, and A. V. Andreev, Phys. Rev. Lett. **94**, 230403 (2005).
[32] Y. Nishida, Ann. Phys. **324**, 897 (2009).
[33] Q. Chen et al., Rep. Prog. Phys. **72**, 122501 (2009).
[34] D. E. Sheehy and L. Radzihovsky, Phys. Rev. Lett. **96**, 060401 (2006); Ann. Phys. **322**, 1790 (2007).